Assembling Structure of Single-Walled Carbon Nanotube Thin Bundles

Jinyong Wang, Zhong Jin, Jin Cheng, and Yan Li*

Beijing National Laboratory for Molecular Sciences, National Laboratory of Rare Earth Material Chemistry and Application, Key Laboratory for the Physics and Chemistry of Nanodevices, College of Chemistry and Molecular Engineering, Peking University, Beijing 100871, China

Received: February 12, 2009; Revised Manuscript Received: March 20, 2009

Atomic force microscopy (AFM), high resolution transmission electron microscopy, and Raman spectroscopy were used to study the assembling structure of thin bundles containing only a few single-walled carbon nanotubes (SWCNTs). The normal close-packed bundles as well as two novel kinds of bundles including spiral bundles and the ribbon-like bundles were observed for both free-standing SWCNTs and SWCNTs on substrates. Molecular mechanics calculation was employed to study the energetic competition between these three types of bundles. It was found that the free-standing spiral bundles and ribbon-like bundles are metastable compared with the close-packed bundles. However, ribbon-like bundles are more likely to be formed on substrates. This indicates that it is not reliable to assess whether the tested nanotube is individual through the height profile of the AFM image.

1. Introduction

Single-walled carbon nanotubes (SWCNTs) have been researched extensively for their unique electronic, optical, and mechanical properties. Because of the strong intertube interaction, which can be as high as 1 eV/nm,[1] the bulk SWCNTs tend to self-assemble into bundles. The bulk SWCNT bundle normally has a triangular lattice structure in a honeycomb array with the uniform intertube spacing of ~0.34 nm.[2−4] This kind of close-packed structure is energetically favorable when the bundle is composed of many tubes. The packing structure greatly affects the properties, especially the mechanical properties of the SWCNTs.

Besides the close-packed large bundles, there are still some small bundles composed of only a few tubes. This kind of bundles exist in the as-prepared SWCNT samples, and more frequently, they are present in the SWCNT dispersions in various solvents.[5−7] SWCNT thin bundles have been found in wide applications. They can act both as the reinforcement materials in SWCNT−polymer composites[8,9] and the high resolution scanning probes.[10,11] SWCNT films on substrate, which are widely used in optoelectronic devices, chemical and biological sensors, field emission devices, and electrodes, are composed of both individual SWCNTs and thin SWCNT bundles.[6,12−14]

Thin SWCNT bundles each containing only a few SWCNTs exist widely. However, studies on such kinds of bundles are still very few. It is well accepted that the properties of nanostructures depend on their structures.[15,16] However, for the thin bundles, their assembling structures are still unclear, let alone how the assembling structures influence the properties. It remains an open question as to whether the SWCNTs in the thin bundles still arrange in a triangular lattice.

In this article, we present a comparison of experimental and theoretical evidence showing that SWCNTs in a thin bundle are not necessarily packed in a triangular lattice. They can assemble into ribbon-like or spiral structures. These kinds of assemblies enriched the aggregation structures of SWCNTs. In addition, the observation of flat ribbon structures composed of a few paralleled SWCNTs indicates that the widely used criterion of individually dispersed SWCNTs by the height measurement with atomic force microscope (AFM) is not reliable.

* To whom correspondence should be addressed. Phone/Fax: +86-10-62756773. E-mail: yanli@pku.edu.cn.

2. Experimental Section

Ultralong SWCNT bundles on substrate were grown on SiO_2/Si substrate by the CVD method at 900 °C. Cu was used as the catalyst and CH_4 as the stock gas.[17] Free-standing SWCNT bundles were directly grown on copper grids coated with SiO_2 using Fe as catalyst and CH_4 (500 sccm) as carbon source at 900 °C.[18] To coat the copper grids with SiO_2, a SiO_2 sol was prepared by mixing together tetraethyl silicate (10 mL), ethanol (30 mL), water (3.5 mL), and 0.5 M HCl (~0.1 mL) and stirring for 2 h. Then the SiO_2 sol was spin-coated onto the copper grids and dried at 80 °C for 30 min before further usage.

Raman measurements were performed under ambient conditions using a helium−neon laser (633 nm, 1.96 eV excitation) in the backscattering configuration on a Jobin-Yvon HR800 spectrometer. The laser power was carefully controlled to avoid sample heating. The AFM images were taken on a SPI3800/SPA400 scanning probe microscope (SEIKO Instruments) with commercial Si cantilevers operated at tapping mode. The high resolution transmission electron microscopy (HRTEM) images were obtained on a Hitachi 9000 TEM.

3. Results and Discussion

Besides the bundles with triangular lattice structure, which are very similar to the bulk assemblies[3,19] and have been observed and studied by many groups in previous studies,[20−22] two new types of SWCNT thin bundles were found in our study. One is of spiral structure, and the other is of ribbon-like structure. Both types have not been reported in the previous study, which may indicate that they only exist in the thin bundles. Figure 1a and b shows the AFM image and the height profile of a thin SWCNT bundle grown on the SiO_2/Si substrate. The periodic fluctuation in its height indicates the spiral structure

10.1021/jp901303b CCC: $40.75
Published on Web 04/15/2009

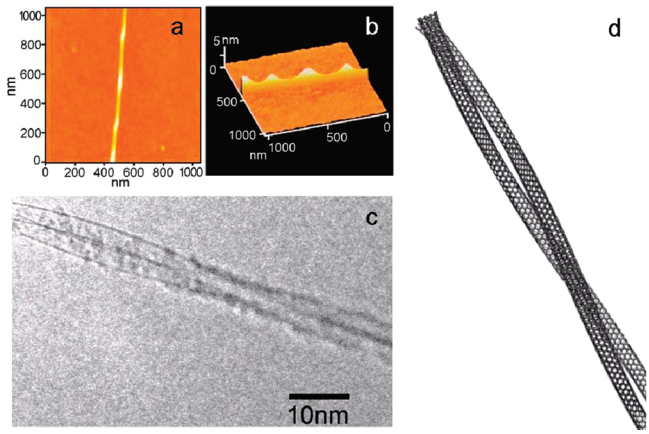

Figure 1. (a and b) AFM image and the corresponding height profile of a spiral bundle on the SiO_2/Si substrate. (c) HRTEM image of a suspended spiral bundle consisting of two tubes. (d) Schematic representation of a spiral bundle.

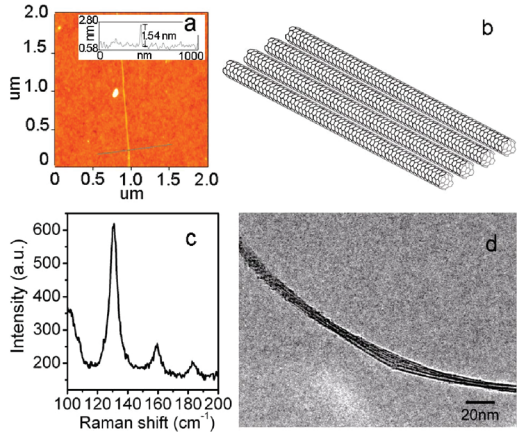

Figure 2. AFM image (a) and Raman spectrum (c) of a ribbon-like bundle on the SiO_2/Si substrate. (b) Schematic representation of a ribbon-like bundle. (d) HRTEM image of a free-standing ribbon-like bundle. The inset image in panel a is the height profile along the line in panel a.

of the bundle. The spiral bundles can also be found in the suspended samples. Figure 1c shows the HRTEM image of a bundle consisting of two tubes that were coiled together. More examples of spiral bundles are shown in Figures S1 and S2 in Supporting Information. Screw pitches larger than 200 nm are often found in the SWCNT samples grown on SiO_2/Si substrates. Screw pitches as small as ~60 nm were found in the free-standing bundles.

Figure 2a shows the AFM image of a ribbon-like thin bundle on the SiO_2/Si substrate. Its height is ~1.54 nm, which is normally accepted as the size of an individual SWCNT. However, three radial breathing mode (RBM) peaks were observed in the Raman spectrum (see Figure 2b). This reveals that it is a bundle containing at least three SWCNTs. The ribbon-like thin bundles also exist in the free-standing SWCNT samples. The HRTEM image in Figure 2d shows a bundle consisting of several tubes assembled in flat structure. More examples of ribbon-like bundles grown on SiO_2/Si substrates are shown in Figure S3 in Supporting Information.

In order to gain more detailed insight into the formation of thin bundles, molecular mechanics simulation was performed on bundles consisting of two SWCNTs, which provides the simplest system to study assembling behavior. Here, four types of spiral bundles were considered, which were composed of two (5, 5) nanotubes, two (7, 7) nanotubes, two (12, 0) nanotubes, and a hybrid bundle of a (7, 7) nanotube and a (12, 0) nanotube. The diameters of (5, 5), (7, 7), and (12, 0) nanotubes were 0.678, 0.949, and 0.939 nm, respectively. For each kind of bundle, the spiral structures with different screw pitches were compared with the corresponding parallel structure. Figure 3 shows the proposed structures of two (5, 5) SWCNTs as an example.

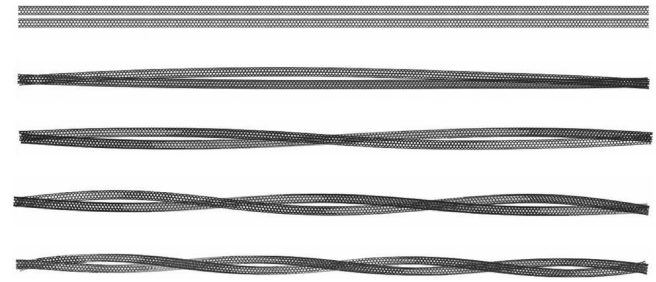

Figure 3. Schematic representations of thin bundles consisting of two (5, 5) nanotubes with different screw pitches: from top to bottom, the parallel bundle and the spiral bundles with screw pitches of 49.2, 36.9, 24.6, and 12.3 nm, respectively. The figure was drawn to scale.

The binding energy was calculated to investigate the driving force for the formation of the different bundles. Here, the binding energy is defined as the energy difference between the bundle and the free-standing individual SWCNTs that composed the bundle. From Figure 4, it can be seen that both the spiral bundles and parallel bundles hold lower energies than the individually presented SWCNTs, which indicates that it is energetically favorable for the SWCNTs to form bundles of different structures. The values of binding energies of the spiral bundles increase with the increase of screw pitches and are always smaller than those of the parallel bundles (Figure 4b). This indicates that the parallel bundles are more stable than the spiral bundles. The spiral structure is metastable in comparison with the stability of the parallel structure.

The binding energy is determined by many factors. At the same screw pitch length, the binding energy value increases with decreasing diameter. The chirality of the SWCNTs also shows influence on the binding energy. For the (12, 0) nanotube, its diameter is slightly smaller than that of the (7, 7) nanotube. However, the value of the binding energy of the spiral bundle containing two (7, 7) nanotubes is larger than that of the spiral bundle containing two (12, 0) nanotubes. The binding energy of a spiral bundle containing a (7, 7) nanotube and a (12, 0) nanotube lies between the above two homogeneous spiral bundles. These facts indicated that it may be more commensurate for some kinds of SWCNTs to form spiral bundles, therefore making stronger intertube interactions. Decreasing the screw pitch will lead to a decrease in the binding energy, especially when the screw pitch is very small. At a large screw pitch, the energy of the spiral structure is very close to that of the parallel bundle. Figures S1 and S2 in the Supporting Information show many examples of spiral bundles with screw pitches larger than 100 nm. In these cases, the binding energy should be very close to that of the parallel bundles.

The binding energy of the bundles rests on two competitive items: (i) the intertube interactions and (ii) the deformation of the tube. The assembling behavior of the tubes depends on the delicate balance between the above two factors. The intertube interaction is determined by the intertube distance and the area of the facing surfaces of the adjacent tubes. Figure 5 shows the pair correlation function $g(r)$ between the carbon atoms of the two individual SWCNTs in a bundle. The pair correlation function $g(r)$ gives the occurrence probability of a carbon atom

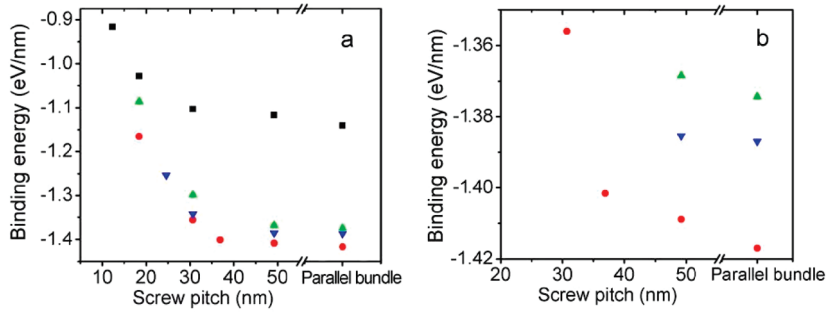

Figure 4. Binding energy of the parallel bundles and the spiral bundles with different screw pitches. The ■, ●, ▲, and ▼ symbols correspond to the bundles consisting of two (5, 5) nanotubes, two (7, 7) nanotubes, two (12, 0) nanotubes, and a hybrid bundle of a (7, 7) nanotube and a (12, 0) nanotube, respectively. Panel b is the magnification of panel a.

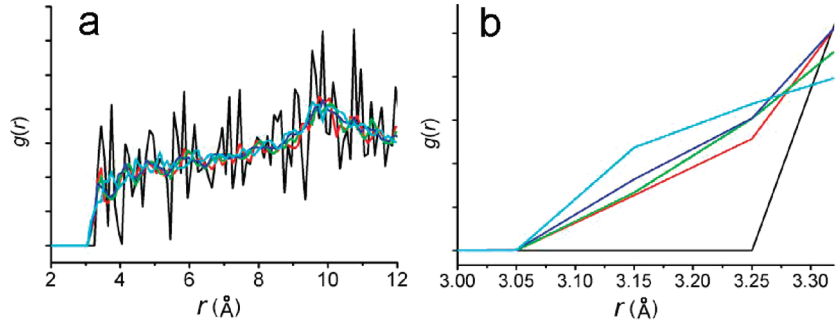

Figure 5. Pair correlation function $g(r)$ between the carbon atoms of the two individual SWCNTs in bundles consisting of two (5, 5) nanotubes with different screw pitches: the parallel bundle (black) and the spiral bundles with screw pitches of 49.2 (red), 36.9 (green), 24.6 (blue), and 12.3 (cyan) nm, respectively. Panel b is the magnification of panel a.

in one nanotube at a distance of r from the carbon atom in the other nanotube. The intertube distance can be inferred from the x-intercept of $g(r)$. The big oscillation in the $g(r)$ of the parallel bundle in Figure 5 is determined by the periodic packing of the bundle along the tube axis. From Figure 5, for the spiral bundles studied, the intertube distances decrease slightly compared to that of the corresponding parallel bundle. The area of the facing surfaces of the two adjacent tubes increases in the spiral bundles accompanied by the deformation of the nanotubes. The slight decrease in the intertube distance and the increase in the facing surface area effectively increases the intertube van der Waals attractions and at the same time lower the energy of the system, while the deformation of the nanotube leads to an energy increase. A decrease in the screw pitch induces rapid binding energy consumption due to the large deformation of the nanotube. When the screw pitch is large, the intertube van der Waals attraction is similar to that of the parallel bundles and the deformation energy is small, which leads to the spiral bundle behavior, which is similar to that of the parallel bundle.

The spiral bundle in the simulation is free of any substrate effects. For the spiral bundle on the substrate, the substrate may play an important role in the assembling of the bundle; due to the interactions between SWCNTs and SiO_2/Si, substrates can be as large as 2−3 eV/nm,[23−25] which are at the same level as the intertube interactions. For the freestanding spiral bundle, our molecular mechanics calculation predicted that the energy of the spiral structure is close to that of the parallel bundle when the screw pitch length is larger than 50 nm (See Figure 4). This value is in good accordance with the observed screw pitch length of ∼60 nm for the freestanding spiral bundle by HRTEM in Figure 1c. However, for spiral bundles on the substrates, the measured screw pitch lengths by AFM normally are larger than 200 nm. We speculate that this is due to the stronger interaction between SWCNTs and SiO_2/Si substrates for parallel bundles than that for the spiral bundle. This hypothesis is further verified by the simulation results. For the spiral bundle, the average distance between the tube and the substrate is larger than that of the parallel bundle on the substrate since some parts of the spiral bundle cannot effectively contact with the substrate. Thus, the binding energy difference of the two kinds of bundles becomes larger on the substrate than that of the freestanding bundles.

A molecular mechanics simulation was further performed on bundles containing three SWCNTs to study the formation of the ribbon-like bundles and the close-packed bundles. Five types of bundles were considered, which are composed of three (5, 5) nanotubes, two (7, 7) nanotubes, and a (12, 0) nanotube, three (7, 7) nanotubes, two (12, 0) nanotubes, and a (7, 7) nanotube, and three (12, 0) nanotubes, respectively. The binding energies for both the ribbon-like bundles and the close-packed bundles are sensitive to the diameter and chirality of the nanotubes. Their binding energy values decrease when increasing the diameter of SWCNTs. The chirality also shows influence on the binding energy due to the different degree of lattice matching between the nanotubes in the bundles. From Figure 6, it can be seen that the binding energy difference between the ribbon-like bundles and the close-packed bundles is larger than 1 eV/nm for the five types of bundles studied; thus, it is always energetically favorable to form close-packed structures. The binding energy is determined by the area of the facing surfaces of the adjacent tubes. The area of the facing surfaces of the close packed bundles is significantly larger than the ribbon-like bundles, which leads to the large binding energy difference between them. The model in the simulation corresponds to free-standing ribbon-like bundles without any substrate effects. This kind of free-standing ribbon-like bundle is metastable. However, concerning the ribbon-like bundles on the substrates, this conclusion may be called into question because of the strong interactions between SWCNTs and the SiO_2/Si substrates. Our molecular mechanics simulation indicates that the ribbon-like

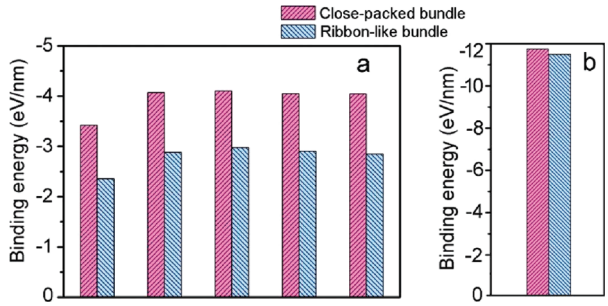

Figure 6. (a) Binding energy of the close-packed bundles and the corresponding ribbon-like bundles consisting of three (5, 5) nanotubes, two (7, 7) nanotubes, and a (12, 0) nanotube, three (7, 7) nanotubes, two (12, 0) nanotubes, and a (7, 7) nanotube, and three (12, 0) nanotubes, respectively, from left to right. (b) Binding energy of the close-packed bundle and the corresponding ribbon-like bundle consisting of three (7, 7) nanotubes on the SiO_2/Si substrates.

bundle composed of three (7, 7) nanotubes on the SiO_2/Si substrate has nearly the same binding energy as that of the close-packed bundle (see Figure 6b). Thus, there should be a big chance for the ribbon-like bundles to form on substrates. For the SWCNTs on substrate, AFM images have been widely used to assess whether the nanotubes are individual or bundled. Our results clearly demonstrate that this method is not very reliable to verify SWCNTs grown on substrates because it cannot distinguish the individual SWCNTs from the ribbon-like bundles by the feature heights.

In summary, SWCNT thin bundles exhibit aggregation behavior different from that of the bulk SWCNT assemblies. Two kinds of novel thin bundles including the spiral bundles and the ribbon-like bundles were observed. The observation of the presence of ribbon-like bundles indicates that AFM height profile is not a reliable method to evaluate whether the nanotubes are individually lain SWCNTs. Molecular mechanics simulation reveals that both the spiral bundles and the ribbon-like bundles were metastable when they are free-standing.

Acknowledgment. This work was supported by the NSF (Projects 50772002 and 90406018) and the MOST (Projects 2006CB932403, 2007CB936202, and 2006CB932701) of China.

Supporting Information Available: AFM images and the corresponding height profiles of three spiral bundles on SiO_2/Si substrates, SEM images of the spiral bundles on SiO_2/Si substrates, AFM images and the Raman spectra of three ribbon-like bundles on the SiO_2/Si substrates, simulation details of the interaction between the nanotube bundle and the SiO_2/Si substrate, and structures of the close-packed bundle and the corresponding ribbon-like bundle consisting of three (7, 7) nanotubes on the SiO_2/Si substrates. This material is available free of charge via the Internet at http://pubs.acs.org.

References and Notes

(1) Girifalco, L. A.; Hodak, M.; Lee, R. S. *Phys. Rev. B* **2000**, *62*, 13104–13110.
(2) Journet, C.; Maser, W. K.; Bernier, P.; Loiseau, A.; de la Chapelle, M. L.; Lefrant, S.; Deniard, P.; Lee, R.; Fischer, J. E. *Nature (London)* **1997**, *388*, 756–758.
(3) Thess, A.; Lee, R.; Nikolaev, P.; Dai, H.; Petit, P.; Robert, J.; Xu, C.; Lee, Y. H.; Kim, S. G.; Rinzler, A. G.; Colbert, D. T.; Scuseria, G. E.; Tománek, D.; Fischer, J. E.; Smalley, R. E. *Science* **1996**, *273*, 483–487.
(4) Ouyang, M.; Huang, J.; Cheung, C. L.; Lieber, C. M. *Science* **2001**, *292*, 702–705.
(5) Islam, M. F.; Rojas, E.; Bergey, D. M.; Johnson, A. T.; Yodh, A. G. *Nano Lett.* **2003**, *3*, 269–273.
(6) Li, Q.; Hao, Y.; Li, X.; Zhang, J.; Liu, Z. *Chem. Mater.* **2002**, *14*, 4262–4266.
(7) Dror, Y.; Pyckhout-Hintzen, W.; Cohen, Y. *Macromolecules* **2005**, *38*, 7828–7836.
(8) Gao, J.; Itkis, M. E.; Yu, A.; Bekyarova, E.; Zhao, B.; Haddon, R. C. *J. Am. Chem. Soc.* **2005**, *127*, 3847–3854.
(9) McIntosh, D.; Khabashesku, V. N.; Barrera, E. V. *J. Phys. Chem. C* **2007**, *111*, 1592–1600.
(10) Cheung, C. L.; Hafner, J. H.; Lieber, C. M. *Proc. Natl. Acad. Sci. U.S.A.* **2000**, *97*, 3809–3813.
(11) Tang, J.; Yang, G.; Zhang, Q.; Parhat, A.; Maynor, B.; Liu, J.; Qin, L.-C.; Zhou, O. *Nano Lett.* **2005**, *5*, 11–14.
(12) Saran, N.; Parikh, K.; Suh, D.-S.; Munoz, E.; Kolla, H.; Manohar, S. K. *J. Am. Chem. Soc.* **2004**, *126*, 4462–4463.
(13) Shi, Y.; Fu, D.; Marsh, D. H.; Rance, G. A.; Khlobystov, A. N.; Li, L.-J. *J. Phys. Chem. C* **2008**, *112*, 13004–13009.
(14) Ding, L.; Tselev, A.; Wang, J.; Yuan, D.; Chu, H.; McNicholas, T. P.; Li, Y.; Liu, J. *Nano Lett.* **2009**, *9*, 800–805.
(15) Kwon, Y.-K.; Saito, S.; Tománek, D. *Phys. Rev. B* **1998**, *58*, R13314−R13317.
(16) López, M. J.; Rubio, A.; Alonso, J. A.; Qin, L.-C.; Iijima, S. *Phys. Rev. Lett.* **2001**, *86*, 3056–3059.
(17) Zhou, W.; Han, Z.; Wang, J.; Zhang, Y.; Jin, Z.; Sun, X.; Zhang, Y.; Yan, C.; Li, Y. *Nano Lett.* **2006**, *6*, 2987–2990.
(18) Jin, Z.; Chu, H.; Wang, J.; Hong, J.; Tan, W.; Li, Y. *Nano Lett.* **2007**, *7*, 2073–2079.
(19) Schlittler, R. R.; Seo, J. W.; Gimzewski, J. K.; Durkan, C.; Saifullah, M. S. M.; Welland, M. E. *Science* **2001**, *292*, 1136–1139.
(20) Hirahara, K.; Saitoh, K.; Yamasaki, J.; Tanaka, N. *Nano Lett.* **2006**, *6*, 1778–1783.
(21) Agnihotri, S.; Mota, J.; Rostam-Abadi, M.; Rood, M. J. *Langmuir* **2005**, *21*, 896–904.
(22) Lu, Q.; Keskar, G.; Ciocan, R.; Rao, R.; Mathur, R. B.; Rao, A. M.; Larcom, L. L. *J. Phys. Chem. B* **2006**, *110*, 24371–24376.
(23) Hertel, T.; Walkup, R. E.; Avouris, P. *Phys. Rev. B* **1998**, *58*, 13870–13873.
(24) Son, H. B.; Samsonidze, G.; Kong, J.; Zhang, Y.; Duan, X. J.; Zhang, J.; Liu, Z. F.; Dresselhaus, M. S. *Appl. Phys. Lett.* **2007**, *90*, 253113–253115.
(25) Zhou, W.; Zhang, Y.; Li, X.; Yuan, S.; Jin, Z.; Xu, J.; Li, Y. *J. Phys. Chem. B* **2005**, *109*, 6963–6967.

JP901303B